Journal of
Computational and Theoretical Nanoscience
Vol. 7, 1–16, 2010

REVIEW

Mathematical Studies and Simulations of Nematic Liquid Crystal Polymers and Nanocomposites

Hong Zhou[1,*], M. Gregory Forest[2], and Hongyun Wang[3]

[1] *Department of Applied Mathematics, Naval Postgraduate School, Monterey, CA 93943, USA*
[2] *Department of Mathematics and Institute for Advanced Materials, University of North Carolina at Chapel Hill, Chapel Hill, NC 27599-3250, USA*
[3] *Department of Applied Mathematics and Statistics, University of California, Santa Cruz, CA 95064, USA*

Nematic liquid crystal polymers and nanocomposites have wide-ranging applications in modern technology including display devices, ultra-fast switches, high strength fibers, and materials with enhanced multi-functional properties including thermal, dielectric, electrical, and barrier properties. In this review article we provide an overview of selected mathematical issues and numerical simulations of nematic liquid crystal polymers and rigid rod nanocomposites. Some open questions will be addressed.

Keywords: Nanocomposites, Nematic Liquid Crystal Polymers, Multifunctional Properties.

CONTENTS

1. INTRODUCTION

Macromolecular materials, in particular, liquid crystalline materials, have a wide range of applications in ultra-fast video displays, temperature and pressure sensors, chromatography and smart fluids for brakes and clutches, high-strength fibers and many more.[95] One prominent example is that nematic liquid crystal polymers have been spun into high strength fibers and then manufactured into special airbags that cushioned the successful landing of NASA's highly publicized missions to Mars.[22]

Peter Palffy-Muhoray has given many interesting examples of liquid crystals in our life in *Physics Today*:[88] "Liquid crystals are all around us: in high strength plastics, snail slime, laundary detergents, textile fibers such as silk and Kevlar, crude oil, insect wings, mineral slurries, lipstick, Bose Einstein condensates, and the mantles of neutron stars. We eat them as aligned molecules in gluten and drink them as phospholipids in milk where they stabilize fat globules. In our bodies they transport fats, make up cell membranes, and affect the functioning of hair cells in the inner ear, and even of DNA." So, what are liquid crystals? Liquid crystallinity refers to a state of matter that is intermediate between the crystalline solid and the amorphous liquid. As a rule, a substance in a liquid crystal state is strongly anisotropic in some of its properties and yet exhibits a certain degree of fluidity. When the concentration of the rodlike molecules is high (lyotropic systems) or when the temperature is low enough (thermotropic systems), the molecules tend to be aligned with each other and the system is in a nematic phase. Otherwise, the molecule orientations are randomly distributed and the system is in an isotropic phase. Figure 1 illustrates the arrangement of rod-like molecules in both the isotropic (or random) phase and the nematic phase. Actually there are many anisotropic mesomorphic phases or mesophases (meaning intermediate phases) with the nematic phase being the simplest one. The orientational order presented in liquid crystals is usually quantified by an order parameter while the orientation of a rodlike molecule is specified by a unit vector along its axis. The nematic liquid crystals have a high degree of long-range orientational order of the molecules but no long-range positional order. This solid–liquid duality leads to many anomalous behaviors of liquid crystalline materials. Liquid crystalline polymers (LCPs) are materials with long and stiff macromolecules, whose conformation and flexibility interact with fluid flows, applied electric or magnetic fields, and thermal conditions. There

*Author to whom correspondence should be addressed.

Report Documentation Page

Form Approved
OMB No. 0704-0188

1. REPORT DATE	2. REPORT TYPE	3. DATES COVERED
2010		**00-00-2010 to 00-00-2010**

4. TITLE AND SUBTITLE	5a. CONTRACT NUMBER
Mathematical Studies and Simulations of Nematic Liquid Crystal Polymers and Nanocomposites	5b. GRANT NUMBER
	5c. PROGRAM ELEMENT NUMBER
6. AUTHOR(S)	5d. PROJECT NUMBER
	5e. TASK NUMBER
	5f. WORK UNIT NUMBER
7. PERFORMING ORGANIZATION NAME(S) AND ADDRESS(ES) **Naval Postgraduate School,Department of Applied Mathematics,Monterey,CA,93943**	8. PERFORMING ORGANIZATION REPORT NUMBER
9. SPONSORING/MONITORING AGENCY NAME(S) AND ADDRESS(ES)	10. SPONSOR/MONITOR'S ACRONYM(S)
	11. SPONSOR/MONITOR'S REPORT NUMBER(S)

12. DISTRIBUTION/AVAILABILITY STATEMENT
Approved for public release; distribution unlimited

13. SUPPLEMENTARY NOTES

14. ABSTRACT

15. SUBJECT TERMS

16. SECURITY CLASSIFICATION OF:			17. LIMITATION OF ABSTRACT	18. NUMBER OF PAGES	19a. NAME OF RESPONSIBLE PERSON
a. REPORT	b. ABSTRACT	c. THIS PAGE			
unclassified	**unclassified**	**unclassified**	**Same as Report (SAR)**	**16**	

are two types of such materials, one called *lyotropic* which is a solution that undergoes a phase transition between isotropic and nematic states when the concentration is increased sufficiently, and the other called *thermotropic* which are melts that exhibit the isotropic to nematic phase transition when the temperature is decreased to a critical temperature. The distinction between lyotropic and thermotropic systems is not crucial for mathematical studies. Products with high tensile modulus are manufactured from these macromolecular materials due to preferred internal molecular orientational order. Understanding the flow of LCPs and the effects of external fields, in particular, the flow-orientational order coupling during material processing, is crucial to predicting new materials with desired properties and to quality control in LCP material processing. Excellent books on this topic include Bird et al.,[3,4] Doi and Edwards,[23] de Gennes,[20] Larson,[67] and Donald et al.[22] A detailed overview on liquid crystals can be found in Ref. [96].

The initial theoretical basis for the rigid rod liquid crystalline polymer is attributed to two Nobel Prize laureates—Lars Onsager and Paul J. Flory. Both the Onsager and Flory theories are statistical theories based on the assumption that liquid crystal phases arise from purely steric

Hong Zhou is an Associate Professor in the Department of Applied Mathematics at Naval Postgraduate School (Monterey, CA). Her major research interests include both numerical and theoretical studies on liquid crystal polymers and nanocomposites. She received her Ph.D. in applied mathematics from the University of California at Berkeley. She was a postdoctoral fellow at the University of North Carolina at Chapel Hill. She taught at the University of California at Santa Cruz for five years before joining the Naval Postgraduate School faculty in 2004.

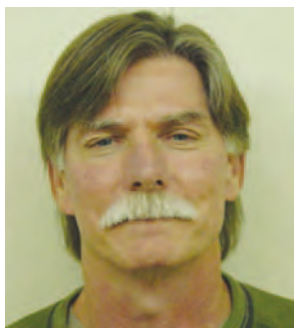

M. Gregory Forest is the Grant Dahlstrom Distinguished Professor of Mathematics and Biomedical Engineering at the University of North Carolina at Chapel Hill. He received his Ph.D. in mathematics from the University of Arizona. He was a full professor at the Ohio State University before he moved to Chapel Hill. Dr. Forest has worked for the past two decades on complex fluids, beginning with fiber spinning and liquid jet models, then branching out to liquid crystal polymers, and more recently biological fluids. The coupling of hydrodynamics, anisotropic microstructure, and boundary conditions lead to challenging mathematical and computational problems that have been the focus of Dr. Forest's work with many colleagues, students and postdocs.

Hongyun Wang is an Associate Professor in the department of Applied Mathematics and Statistics at University of California, Santa Cruz (UC Santa Cruz). He obtained his B.S. and M.S. degrees in Mathematics at Beijing University, China, and obtained his Ph.D. in Mathematics at University of California, Berkeley (UC Berkeley) in 1996, under the supervision of Professor Alexandre J. Chorin and with a dissertation in Fluid Dynamics. While finishing his Ph.D., he got interested in Biophysics, and in particular, the force generation mechanism of molecular motors. After finishing his Ph.D., he changed his research into the area of modeling molecular motors. In 1996–1999, he worked as a postdoctoral fellow in the group of Professor George F. Oster, in the department of Molecular and Cellular Biology at UC Berkeley. While working with Oster's group, he proposed the binding zipper model, which explains how ATP binding free energy is utilized gradually and efficiently to generate a nearly constant force at the catalytic site. In 1999, he joined the School of Engineering at UC Santa Cruz, as Assistant Professor. At UC Santa Cruz, he continued his research on molecular modeling. He proposed the Stokes efficiency, which measures how efficiently a motor is using the chemical free energy to drive through the viscous media. He proposed using motor potential profile to represent the overall motor operation and designed a robust formulation for extracting motor potential profile from experimental date. Recently he got interested in studying polymer problems in the rigorous mathematical framework of non-linear Smoluchowski equation. At UC Santa Cruz, he was a founding member of, and was actively involved in establishing the department of Applied Mathematics and Statistics. In 2005, he was promoted to Associate Professor with tenure.

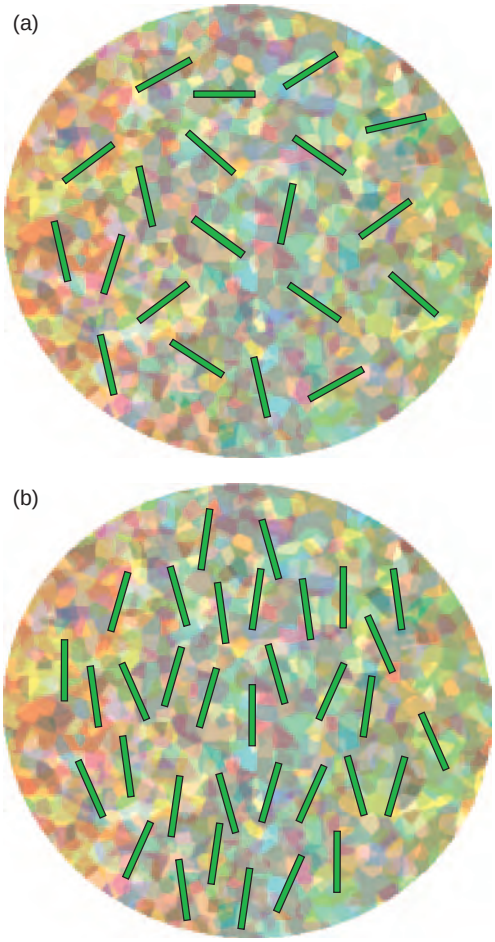

Fig. 1. The arrangement of rod-like molecules (a) in the isotropic phase; (b) in the nematic phase.

interactions. The main difference between the two theories is that the Onsager theory uses the second virial expansion of the interaction energy whereas the Flory theory uses the lattice model to simulate the excluded volume effect. Because of its virial expansion, the Onsager theory is more applicable to dilute solutions. Introducing higher virial terms may extend the Onsager theory to concentrated solutions.[59, 60] In contrast, the Flory theory makes some assumptions valid only in a perfectly ordered phase. These assumptions restrict the Flory theory to high concentrations and a highly ordered phase. Both the Onsager and Flory theories predict an isotropic–nematic phase transition when the polymer concentration is sufficiently high (or equivalently when the temperature is sufficiently low).

The Leslie-Ericksen (LE) vector theory[24, 73] is one of the earliest constitutive theories of liquid–crystals. It extends Oseen and Frank's continuum theory of elasticity of liquid crystals at rest to model flow behavior.[44] The LE model takes the microstructure of the material into account by postulating a unit "director" that characterizes the direction of local ordering of the polymer rods. The theory assumes a uniquely defined principal axis exists everywhere. The LE model has been successfully applied to studying the flow of nematic rod dispersions of low molar–mass.[20] Since it assumes the linear dependence of the stress tensor on the deformation rate, the LE theory is limited to low deformation rates and cannot describe nonlinear rheological properties, such as the shear thinning of the viscosity of LCPs. Since the theory also assumes an identifiable principal direction of orientation everywhere, it must be extended to resolve singularities which must arise in the core of topological defects. This work has a rich history which the reader can find in some excellent manuscripts on the subject.[63, 64, 103]

Kinetic theories for liquid–crystalline polymers based on the dynamics of the nonequilibrium orientational distribution function have been developed by Siegfried Hess[47] and Masao Doi.[23] The basic idea behind the Doi–Hess theory is to treat the LCP as a suspension of rigid rodlike nematogenic molecules and describe the ensemble with an orientational probability density function (pdf). The orientational pdf evolves according to a nonlinear Smoluchowski (Fokker-Planck) equation where the forces acting on the rodlike molecules include hydrodynamic, Brownian and intermolecular forces. The orientational order present in a nematic LCP derives from intermolecular forces of various origins. Such molecular interactions are represented in the Smoluchowski equation by a mean-field potential known as the nematic potential. The two commonly used intermolecular potentials are the Onsager potential and the Maier-Saupe potential. The Onsager potential is based on excluded-volume interactions of a single rigid rodlike test molecule with the other surrounding molecules. The Onsager potential can be written as

$$V_{\text{Onsager}}(\mathbf{m}) = \nu k_{\text{B}} T \int_{|\mathbf{m}'|=1} \beta(\mathbf{m}, \mathbf{m}')\rho(\mathbf{m}')\, d\mathbf{m}' \quad (1)$$

where $\mathbf{m}$ and $\mathbf{m}'$ are unit vectors, $\rho(\mathbf{m})$ denotes the probability density function that a random molecule in the ensemble has orientation $\mathbf{m}$ at time t, $\beta(\mathbf{m}, \mathbf{m}') = 2dL^2|\mathbf{m} \times \mathbf{m}'|$ represents the excluded-volume interaction between two rodlike molecules with orientations $\mathbf{m}$ and $\mathbf{m}'$, ν is the number density of the rigid rodlike molecules with diameter d and length L, k_{B} is the Boltzmann constant, and T is temperature. One can approximate the magnitude of the cross product by the following expression:

$$\begin{aligned} |\mathbf{m} \times \mathbf{m}'| &= \sqrt{\sin^2 \Theta} = \sqrt{1 - \cos^2 \Theta} \\ &\approx 1 - \frac{1}{2}\cos^2 \Theta = 1 - \frac{1}{2}(\mathbf{m} \cdot \mathbf{m}')^2 \end{aligned} \quad (2)$$

where Θ is the angle between $\mathbf{m}$ and $\mathbf{m}'$. Using the above approximation, one can simplify the Onsager potential to the Maier-Saupe potential:

$$V_{\text{MS}} = -\frac{3Uk_{\text{B}}T}{2}\mathbf{mm} : \mathbf{M} \quad (3)$$

REVIEW

where U is the nematic strength, and $\mathbf{M}$ is the second moment of the orientation distribution

$$\mathbf{M} \equiv \langle \mathbf{mm} \rangle = \int_{|\mathbf{m}|=1} \mathbf{mm}\rho(\mathbf{m})\, d\mathbf{m} \tag{4}$$

The Maier-Saupe potential (3) was originally developed for studying phase transitions in thermotropic liquid crystals and it has been widely adopted in the study of liquid crystalline polymers. The Maier-Saupe is analytically less complicated in that it is completely specified by the second moment. In contrast, the Onsager potential depends on the whole pdf.

The fact that the Maier-Saupe potential is completely specified by the second moment also inspires a further simplification in which the Smoluchowski equation is approximated by an equation for the second moment. As a result, the macroscopic properties of interest at any material point depend not on the distribution function ρ directly, but rather on low moments of ρ. Indeed, this projection is how one makes contact with the Landau-deGennes approach which is to posit closed equations, the free energy, and stress constitutive law explicitly in terms of the second moment of the pdf. Below we review briefly the approach of closure approximation. This approach has been widely adopted in the development of numerical methods for solving the closure-based class of problems for dilute polymer solutions (e.g., "Boger fluids") and other complex fluids including liquid crystal polymers. For simplicity, here *we restrict ourselves to the two-dimensional Doi–Hess theory in the absence of flow*.

We parametrize the rod axis by $\mathbf{m} = (m_1, m_2)$. Let θ be the angular coordinate of $\mathbf{m}$. We have

$$\begin{aligned} &m_1 = \cos\theta, \quad m_2 = \sin\theta \\ &\frac{\partial m_1}{\partial \theta} = -m_2, \quad \frac{\partial m_2}{\partial \theta} = m_1 \end{aligned} \tag{5}$$

The stochastic evolution of one polymer rod is described by a Langevin equation:[70]

$$d\theta = -D\frac{V'(\theta)}{k_{\mathrm{B}}T}dt + \sqrt{2D}\cdot dW \tag{6}$$

where D is the diffusion constant, $V(\theta)$ is the total potential including the intermolecular potential and other potentials in the absence of external fields, and $W(t)$ is the Wiener process (Brownian motion). In general, the Langevin equation approach is limited because of the nonlocality of the excluded volume potential, but more so because there are many degeneracies due to rotational invariance of equilibria, and in shear flow there are many limit cycles and bifurcations which are, thus far, not detectable from statistics of stochastic differential equation paths. One popular approach is to use a mesoscopic probability density function to describe the molecules and then use the Maier-Saupe potential which gives the interaction potential between a (test) polymer rod and the surrounding polymer rods described by mesoscopic probability density.

The Maier-Saupe potential can be expressed as

$$V_{\mathrm{MS}} = -\frac{3Uk_{\mathrm{B}}T}{2}\mathbf{mm}:\left(\mathbf{M}-\frac{\mathbf{I}}{2}\right) = -2Nk_{\mathrm{B}}T\,\mathbf{mm}:\mathbf{Q} \tag{7}$$

where $N = 3U/4$, and $\mathbf{Q}$ is the orientation tensor (traceless normalization of the second moment)

$$\mathbf{Q} \equiv \langle \mathbf{mm} \rangle - \frac{\mathbf{I}}{2} = \begin{bmatrix} Q_{11} & Q_{12} \\ Q_{21} & Q_{22} \end{bmatrix} \tag{8}$$

The orientation tensor $\mathbf{Q}$ is symmetric and traceless, so $Q_{12} = Q_{21}$ and $Q_{11} = -Q_{22}$.

The probability density function $\rho(\theta, t)$ is described by the Smoluchowski equation

$$\frac{\partial \rho}{\partial t} = D_{\mathrm{r}}\frac{\partial}{\partial \theta}\left(\frac{V'_{MS}(\theta)}{k_{\mathrm{B}}T}\rho + \frac{\partial \rho}{\partial \theta}\right) \tag{9}$$

where D_{r} is the rotational diffusion coefficient of polymer rods. For simplicity we set $D_{\mathrm{r}} = 1$, which is equivalent to a re-scaling of time for constant D_{r}; the more general orientation-dependent diffusion constant does not lead to qualitatively different results. To derive an equation for the orientation tensor, we first use (5) to derive the identity:

$$\begin{aligned} &\left\langle \frac{\partial}{\partial \theta}(\mathbf{mm})\left(\frac{\partial}{\partial \theta}(\mathbf{mm}):\mathbf{Q}\right)\right\rangle \\ &\quad = \langle -4(\mathbf{mm})((\mathbf{mm}):\mathbf{Q}) + 4(\mathbf{mm})\cdot\mathbf{Q}\rangle \end{aligned} \tag{10}$$

The proof of this equation is straightforward. We first show that the $(1,1)$-component is the same for both sides even before taking the average.

$$\begin{aligned} &\left\{\frac{\partial}{\partial \theta}(\mathbf{mm})\left[\frac{\partial}{\partial \theta}(\mathbf{mm}):\mathbf{Q}\right]\right\}_{1,1} \\ &= -2m_1m_2[-2m_1m_2(Q_{11}-Q_{22}) + 2(m_1^2-m_2^2)Q_{12}] \\ &= -4m_1^2[(-m_2^2)Q_{11} + m_2^2Q_{22}] - 4m_1m_2(2m_1^2-1)Q_{12} \\ &= -4m_1^2[m_1^2Q_{11} + m_2^2Q_{22}] + 4m_1^2Q_{11} \\ &\quad - 4m_1^2[2m_1m_2Q_{12}] + 4m_1m_2Q_{12} \\ &= -4\{(\mathbf{mm})[(\mathbf{mm}):\mathbf{Q}]\}_{1,1} + 4\{(\mathbf{mm}):\mathbf{Q}\}_{1,1} \end{aligned} \tag{11}$$

Next we check the $(1,2)$-component.

$$\begin{aligned} &\left\langle \frac{\partial}{\partial \theta}(\mathbf{mm})\left[\frac{\partial}{\partial \theta}(\mathbf{mm}):\mathbf{Q}\right]\right\rangle_{1,2} \\ &= \langle (m_1^2-m_2^2)[-2m_1m_2(Q_{11}-Q_{22}) + 2(m_1^2-m_2^2)Q_{12}]\rangle \\ &= \langle -4m_1m_2(m_1^2-m_2^2)Q_{11} + 2(m_1^2-m_2^2)^2Q_{12}\rangle \end{aligned} \tag{12}$$

On the other hand,

$$\langle -4(\mathbf{mm})[(\mathbf{mm}):\mathbf{Q}] + 4(\mathbf{mm}):\mathbf{Q}\rangle_{1,2}$$

$$
\begin{aligned}
&= \langle -4(m_1m_2)(m_1^2Q_{11}+m_2^2Q_{22}+2m_1m_2Q_{12}) \\
&\quad +4(m_1^2Q_{12}+m_1m_2Q_{22})\rangle \\
&= \langle -4m_1m_2(m_1^2-m_2^2)Q_{11}+2(m_1^2-m_2^2)Q_{12}\rangle \\
&\quad +\langle 2(2m_1^2-1)Q_{12}+4m_1m_2Q_{22}\rangle \\
&= \langle -4m_1m_2(m_1^2-m_2^2)Q_{11}+2(m_1^2-m_2^2)Q_{12}\rangle \\
&\quad +\langle 2(m_1^2-m_2^2)Q_{12}+4m_1m_2Q_{22}\rangle \\
&= \langle -4m_1m_2(m_1^2-m_2^2)Q_{11}+2(m_1^2-m_2^2)Q_{12}\rangle \\
&\quad +\langle 2(m_1^2-m_2^2)\rangle Q_{12}+\langle 4m_1m_2\rangle Q_{22} \\
&= \langle -4m_1m_2(m_1^2-m_2^2)Q_{11}+2(m_1^2-m_2^2)Q_{12}\rangle \\
&\quad +2(Q_{11}-Q_{22})Q_{12}+4Q_{12}Q_{22} \\
&= \langle -4m_1m_2(m_1^2-m_2^2)Q_{11}+2(m_1^2-m_2^2)Q_{12}\rangle \\
&\quad -4Q_{22}Q_{12}+4Q_{12}Q_{22} \\
&= \langle -4m_1m_2(m_1^2-m_2^2)Q_{11}+2(m_1^2-m_2^2)Q_{12}\rangle \qquad (13)
\end{aligned}
$$

This completes the proof.

Combining the identity (10) with Smoluchowski equation (9), we find

$$
\begin{aligned}
\frac{d\mathbf{Q}}{dt} &= \frac{d\langle \mathbf{mm}\rangle}{dt} = \int_{|\mathbf{m}|=1}(\mathbf{mm})\frac{\partial \rho}{\partial t}\,d\theta \\
&= \int_{|\mathbf{m}|=1}(\mathbf{mm})\frac{\partial}{\partial \theta}\left[\frac{\partial \rho}{\partial \theta}+\frac{\rho}{k_BT}\frac{\partial V_{MS}}{\partial \theta}\right]d\theta \\
&= -\int_{|\mathbf{m}|=1}\frac{\partial}{\partial \theta}(\mathbf{mm})\left(\frac{\partial \rho}{\partial \theta}+\frac{\rho}{k_BT}\frac{\partial V_{MS}}{\partial \theta}\right)d\theta \\
&= \int_{|\mathbf{m}|=1}\frac{\partial^2}{\partial \theta^2}(\mathbf{mm})\rho\,d\theta \\
&\quad +2N\int_{|\mathbf{m}|=1}\frac{\partial}{\partial \theta}(\mathbf{mm})\left[\frac{\partial}{\partial \theta}(\mathbf{mm}):\mathbf{Q}\right]\rho\,d\theta \\
&= \int_{|\mathbf{m}|=1}(2\mathbf{I}-4\mathbf{mm})\rho\,d\theta \\
&\quad +2N\int_{|\mathbf{m}|=1}(-4(\mathbf{mm})[(\mathbf{mm}):\mathbf{Q}]+4(\mathbf{mm})\cdot\mathbf{Q})\rho\,d\theta \\
&= 2\mathbf{I}-4\langle \mathbf{mm}\rangle-8N\langle \mathbf{mmmm}\rangle:\mathbf{Q}+8N\langle \mathbf{mm}\rangle\cdot\mathbf{Q} \\
&= -4\mathbf{Q}+8N\left(\mathbf{Q}+\frac{\mathbf{I}}{2}\right)\cdot\mathbf{Q}-8N\langle \mathbf{mmmm}\rangle:\mathbf{Q} \qquad (14)
\end{aligned}
$$

Therefore, we have derived

Orientation tensor model:

$$
\frac{d\mathbf{Q}}{dt} = -4\mathbf{Q}+8N\left(\mathbf{Q}+\frac{\mathbf{I}}{2}\right)\cdot\mathbf{Q}-8N\langle \mathbf{mmmm}\rangle:\mathbf{Q} \qquad (15)
$$

In (15), the evolution of $\mathbf{Q}$ is affected by the fourth moment $\langle \mathbf{mmmm}\rangle$. The coupling between moments in (15) requires some closure approximation. The quadratic Doi closure rule assumes

Doi closure:

$$
\begin{aligned}
\langle \mathbf{mmmm}\rangle:(\bullet) &= \langle \mathbf{mm}\rangle\langle \mathbf{mm}\rangle:(\bullet) \\
&= \mathbf{MM}:(\bullet)=(\mathbf{M}:(\bullet))\mathbf{M}
\end{aligned} \qquad (16)
$$

Different closure rules, such as Hinch-Leal,[52] Tsuji-Rey,[94] have been studied. We list some 2D closure rules below.

Tsuji-Rey closure:

$$
\begin{cases}
\langle \mathbf{mmmm}\rangle:(\bullet)=\dfrac{1}{4}\Big[(\mathbf{Q}:(\bullet))\mathbf{Q}+\mathbf{Q}^2\cdot(\bullet) \\
\qquad +\mathbf{Q}\cdot(\bullet)\cdot\mathbf{Q}+(\bullet)\cdot\mathbf{Q}^2 \\
\qquad -((\mathbf{Q}\cdot(\bullet)):\mathbf{Q})\mathbf{I}+\dfrac{1}{2}(\mathbf{Q}:(\bullet))\mathbf{I}\Big]
\end{cases} \qquad (17)
$$

Hinch-Leal 1 closure:

$$
\begin{cases}
\langle \mathbf{mmmm}\rangle:(\bullet)=\dfrac{1}{5}[6\mathbf{M}\cdot(\bullet)\cdot\mathbf{M}-(\bullet):(\mathbf{MM}) \\
\qquad -2((\bullet):\mathbf{MM}-(\bullet):\mathbf{M})\mathbf{I}]
\end{cases} \qquad (18)
$$

Hinch-Leal 2 closure:

$$
\begin{cases}
\langle \mathbf{mmmm}\rangle:(\bullet)=\mathbf{M}((\bullet):\mathbf{M}) \\
\qquad +2[\mathbf{M}\cdot(\bullet)\cdot\mathbf{M}-\mathbf{M}^2((\bullet):\mathbf{M}^2)/(\mathbf{I}:\mathbf{M}^2)] \\
\qquad +\alpha(\mathbf{M})\Big\{\dfrac{52}{315}(\bullet)-\dfrac{8}{21}[(\bullet)\cdot\mathbf{M} \\
\qquad\qquad +\mathbf{M}\cdot(\bullet)-((\bullet):\mathbf{M})\mathbf{I}]\Big\} \\
\qquad \text{where } \alpha(\mathbf{M})=\exp[2(\mathbf{I}-3\mathbf{M}^2:\mathbf{I})/(\mathbf{I}-(\bullet):\mathbf{M}^2)\mathbf{I}]
\end{cases} \qquad (19)
$$

Detailed studies on closure rules can be found in Ref. [28]. As illustrated here, the orientation tensor theory is either derived or recovered from the kinetic theory for the density function by projection onto a second-moment description using closure rules.

To give a more mathematical description on the orientation tensor $\mathbf{Q}$, let us temporarily leave 2D rods in favor of 3D rods. The orientation tensor $\mathbf{Q}$ is the basis for micron-scale light scattering measurements of primary axes (directors), degrees of molecular alignment (birefringence), and normal and shear stress measurements. The spectral representation of $\mathbf{Q}$ gives mesoscopic directors and order parameters. In three-dimensional space (3D) the eigenvalues of $\mathbf{Q}$, $d_i-1/3$, are the order parameters, which describe the averaged degrees of orientation with respect to the eigenvectors of $\mathbf{Q}$, $\mathbf{n}_i$, which in turn are the mesoscopic principal optical axes. The ellipsoid of Figure 2 depicts a geometric representation of the orientation tensor $\mathbf{Q}$ in 3D space.

An experimentalist can probe the optical axes by varying the plane transverse to the light signal; the principal axes corresponds to a plane with local maximal birefringence (or anisotropy). Birefringence in the plane of $\mathbf{n}_i$, $\mathbf{n}_j$ (or any plane) is measured by differences in the principal degrees of orientation, $B_{ij}=|d_i-d_j|$. We further note that $d_i>1/3$ implies that on an average the molecules align

REVIEW

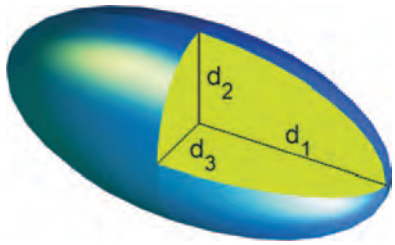

Fig. 2. A geometric representation of the mesoscale 3D orientation tensor **Q**. The axes lengths d_i's are given by eigenvalues $(d_i - 1/3)$ of the symmetric matrix **Q**, whereas the axes are determined by the orthonormal frame of eigenvectors of **Q**.

toward the principal axis $\mathbf{n}_i$, whereas $d_i < 1/3$ implies greater alignment with the plane perpendicular to $\mathbf{n}_i$. The principal axis associated with the largest value of d_i is usually referred as the "major director." Mathematically, a spectral representation of **Q** is given by

$$\mathbf{Q} = \sum_{i=1}^{3} \left(d_i - \frac{1}{3} \right) \mathbf{n}_i \otimes \mathbf{n}_i$$

$$\sum_{i=1}^{3} d_i = 1$$

$$d_i = \langle \mathbf{n}_i \dot{\mathbf{m}} \rangle = \langle \cos^2 \langle \mathbf{n}_i \dot{\mathbf{m}} \rangle \rangle$$

where $\langle \mathbf{n}_i \dot{\mathbf{m}} \rangle$ is the angle between the directors $\mathbf{n}_i$ and $\mathbf{m}$. The isotropic state corresponds to the case where $d_1 = d_2 = d_3 = 1/3$ or equivalently $\mathbf{Q} = \mathbf{0}$, and the ellipsoid of Figure 2 reverts to a sphere with random mesoscale order.

In the presence of flow field, the probability density function $\rho(\mathbf{m}, \mathbf{x}, t)$ is governed by the Smoluchowski equation below, in which the time has been re-scaled with the rotational diffusion coefficient.

Smoluchowski equation:

$$\frac{D\rho}{Dt} = \mathscr{R} \cdot (\rho \mathscr{R} \mu) - \mathscr{R} \cdot (\mathbf{m} \times \dot{\mathbf{m}} \rho) \tag{20}$$

In (20), $D/Dt = \partial/\partial t + \mathbf{v} \cdot \nabla$ denotes the material time derivative, $\mu(\mathbf{m}) = \ln \rho(\mathbf{m}) + V(\mathbf{m})/k_B T$ is the normalized chemical potential density, $\mathscr{R} = \mathbf{m} \times \partial/\partial \mathbf{m}$ is the rotational gradient operator, and $\dot{\mathbf{m}}$ is the Jeffery orbit of ellipsoids given by

$$\dot{\mathbf{m}} = \Omega \cdot \mathbf{m} + a(\mathbf{D} \cdot \mathbf{m} - \mathbf{D} : \mathbf{mmm}) \tag{21}$$

In (21), **D** and Ω are the rate-of-strain and vorticity tensors, and a is the aspect ratio parameter defined as $a = (r^2+1)/(r^2-1)$ where r is the ratio of the rod length or plate thickness to the diameter. $0 < a \leq 1$ corresponds to the case of rod-like molecules and $-1 \leq a < 0$ for the case of platelets. In the presence of external electric/magnetic fields, the potential $V(\mathbf{m})$ in $\mu(\mathbf{m})$ above will include terms in addition to the Maier-Saupe potential.

The development of the Doi–Hess theory has given a large impetus to the study of rheology of liquid–crystalline polymers. For planar linear flows the monodomain problem has been solved.[37] What remains open is full 3D linear flows.

2. MATHEMATICAL STUDIES OF PURE NEMATICS

The isotropic–nematic (I–N) phase transition in hard rod gases and liquids is a classical topic, which was first explained theoretically by Onsager in terms of excluded volume potential.[87] Onsager's approach was based on a variational model where the second virial coefficient was calculated for excluded volume interaction between the rods. His calculation resulted in a non-analytic $|\mathbf{m} \times \mathbf{m}'|$ potential where **m** represents the direction of the rod. Later Maier and Saupe (3) re-examined the I–N transition with a simpler potential in the form of $-(\mathbf{m} \cdot \mathbf{m}')^2$ that now bears their names.[80] The Maier-Saupe potential is a quartic approximation of the Onsager potential, which affords sufficient degrees of freedom to capture the hysteresis loop in an order parameter representation of isotropic and anisotropic equilibria. The interaction employed in the Maier-Saupe theory of the nematic state has been generalized in a manner consistent with the asymmetry of the molecules that exhibit a nematic phase.[45] The bifurcation in Onsager's model of the isotropic–nematic transition in a three-dimensional system of hard rods as well as the corresponding two-dimensional system of hard lines was investigated in Ref. [58]. It was found that the existence and order of a phase transition depend on both the direction of bifurcation and on properties of the global solutions. In 1986 Doi and Edwards[23] employed a second-moment closure approximation for the Smoluchowski equation for the probability density function (PDF) to further illustrate robustness of the I–N transition with coarse-grained models and an excluded-volume potential. In Ref. [40] a simple proof was given to show that all steady states of the Doi–Hess tensor model are unaxial. In fact, the homogeneous nematic dynamics of liquid crystalline polymers without flow is described by the following Doi–Hess orientation tensor model:

$$\frac{d}{dt}\mathbf{Q} = -F(\mathbf{Q}) \tag{22}$$

Here

$$F(\mathbf{Q}) = \left(1 - \frac{N}{3}\right)\mathbf{Q} - N(\mathbf{Q} \cdot \mathbf{Q}) + N(\mathbf{Q} : \mathbf{Q})\left(\mathbf{Q} + \frac{\mathbf{I}}{3}\right) \tag{23}$$

where **Q** is a second-order, symmetric, traceless tensor that describes the average molecular orientation with respect to a probability distribution, N is the dimensionless polymer concentration that dictates the strength of the Maier-Saupe potential. The orientation tensor **Q** is said to have *uniaxial* symmetry if two of its eigenvalues are identical; otherwise, it is said to exhibit *biaxial* symmetry. In order to show that all homogeneous equilibria of (22) are uniaxial, we first

diagonalize the equation $F(\mathbf{Q}) = 0$ using orthogonal frame of eigenvectors of $\mathbf{Q}$. Then we show that all three eigenvalues of $\mathbf{Q}$ satisfy a quadratic equation; therefore there are at most two distinct eigenvalues out of three, which is the definition of uniaxiality. However, the dynamics of the orientation tensor $\mathbf{Q}$ is not necessarily uniaxial. The stability of each steady state was examined in full system in Ref. [40].

The proof that all kinetic model equilibria are uniaxial is much harder and remained open until quite recently, when mathematical analysts, led by Constantin, Kevrekidis and Titi,[13–15] began to revisit Onsager's seminal papers and provide modern rigorous proofs about stationary solutions.

In Refs. [14, 15, 26, 77] the authors conducted a detailed study of the 2-D model where the rod orientation is confined to a unit circle. In Ref. [13] Constantin et al. also considered the 3-D model where the rod orientation lies on a unit sphere. They provided an upper bound on the number of critical points from the analysis of a transcendental equation for the orientational order tensor. However, a complete classification of all equilibria was not addressed. Incidentally, it was in 2005 that three different proofs appeared to show that all anisotropic equilibrium solutions of the Smoluchowski equation must be axial symmetric on a sphere with Maier-Saupe interaction potential.[25, 75, 115] In both Refs. [25 and 75] the proof of the axial symmetry was based on spherical harmonics expansions. Stability of critical points with Maier-Saupe interaction potential was also considered in Ref. [25] without details. Very recently in Ref. [106] the axial symmetry of several different cases, including pure nematic polymers, dipolar nematic polymers and polymers in higher dimensional space, was unified by a key inequality. In the following we are going to briefly summarize these different proofs. For more details, see the Refs. [25, 75, 106, 115].

In Ref. [25] Fatkullin and Slastikov provided a rigorous analysis and classification of all critical points of Onsager's functional. The Onsager free energy functional can be expressed as the sum of an entropic term and an interaction term and it has the expression

$$F[\rho] = \int_{S^2} \left[T\rho(s)\ln\rho(s) + \frac{1}{2}\rho(s)\int_{S^2} U(s,s')\rho(s')\,ds' \right] ds \quad (24)$$

where $\rho(s)$ is a probability density function describing rod orientations for a system of liquid–crystalline suspensions, s is the orientation parameter which lies on a unit sphere S^2, T is the temperature (and the Boltzmann constant k_B is set to unity), and $U(s,s')$ is the Maier-Saupe potential. The uniform density $\bar{\rho} = 1/4\pi$ describes the isotropic phase where the molecules are randomly oriented. The main result in Ref. [25] is that the uniform density is a unique critical point when $T > T^* \approx 0.149$ and an isolated minimizer for $T > T_c = 2/15$. At $T = T^*$ a saddle-node bifurcation occurs. The important tool used in Ref. [25] is the spherical harmonics. Similar approach has been used in Ref. [75].

In Ref. [115] we provided a proof based on elementary calculus. In the absence of external field and flow, the governing equation for stiff rod nematic polymers interacting by the Maier-Saupe potential is given by the Smoluchowski (or Fokker-Planck) equation:

$$\begin{aligned} \frac{\partial\rho}{\partial t} &= D\frac{\partial}{\partial\mathbf{u}}\cdot\left(\frac{1}{k_B T}\frac{\partial V}{\partial\mathbf{u}}\rho + \frac{\partial\rho}{\partial\mathbf{u}}\right) \\ V(\mathbf{u},[\rho]) &= -bk_B T(\mathbf{u}\otimes\mathbf{u}) : \langle\mathbf{u}\otimes\mathbf{u}\rangle \\ \langle\mathbf{u}\otimes\mathbf{u}\rangle &= \int_S (\mathbf{u}\otimes\mathbf{u})\rho(\mathbf{u})\,d\mathbf{u} \end{aligned} \quad (25)$$

where ρ is the orientational distribution function, $\mathbf{u}$ a unit vector specifying the orientation of a rodlike molecule, D the rotational diffusion coefficient, V the Maier-Saupe short-range nematic potential, $\langle\mathbf{u}\otimes\mathbf{u}\rangle$ the second moment of ρ, k_B the Boltzmann constant, T the absolute temperature, and b the strength of the nematic potential. In equilibrium the solution of the Smoluchowski equation is given by the Boltzmann distribution:

$$\rho(\mathbf{u}) = \frac{\exp(-V(\mathbf{u},[\rho]))}{\int_S \exp(-V(\mathbf{u},[\rho]))\,d\mathbf{u}} \quad (26)$$

Since $\langle\mathbf{u}\otimes\mathbf{u}\rangle$ is symmetric, we choose a Cartesian system such that $\langle\mathbf{u}\otimes\mathbf{u}\rangle$ is diagonal:

$$\langle\mathbf{u}\otimes\mathbf{u}\rangle = \begin{pmatrix} \frac{1}{3}+r_1 & 0 & 0 \\ 0 & \frac{1}{3}+r_2 & 0 \\ 0 & 0 & \frac{1}{3}+r_3 \end{pmatrix} \quad (27)$$

where $\mathbf{u} = (u_1, u_2, u_3)$ and $r_i = \langle u_i^2\rangle - 1/3$. If $r_1 = r_2 = r_3 = 0$, then the system is in isotropic state; If there are two distinct eigenvalues among r_1, r_2 and r_3, then the system is in axisymmetric (uniaxial) state. Upon diagonalization of the second moment $\langle\mathbf{u}\otimes\mathbf{u}\rangle$, the probability distribution function takes a simple form:

$$\rho(\mathbf{u}) = \frac{\exp[b(r_1u_1^2 + r_2u_2^2 + r_3u_3^2 + 1/3)]}{\int_S \exp[b(r_1u_1^2 + r_2u_2^2 + r_3u_3^2 + 1/3)]\,d\mathbf{u}} \quad (28)$$

where b is treated as a variable for mathematical convenience. Then we introduce three random variables:

$$h_i = u_i^2 - \langle u_i^2\rangle, \quad i = 1, 2, 3 \quad (29)$$

and show that they have following properties:

1. $\langle h_i\rangle = 0$, $i = 1, 2, 3$; $\sum_{i=1}^3 h_i = 0$.
2. Suppose $r_1 > r_2$. Then for $b > 0$, we have $\langle h_3(h_1 - h_2)\rangle < 0$. Note that $\langle h_3h_1\rangle$ is the correlation of u_3^2 and u_1^2 while $\langle h_3h_2\rangle$ is the correlation of u_3^2 and u_2^2.

REVIEW

We further define functions

$$R_i(b) = \langle u_i^2 \rangle - \frac{1}{3}, \quad i = 1, 2, 3 \tag{30}$$

which satisfy

1. $R_i(0) = 0$, $i = 1, 2, 3$
2. If (r_1, r_2, r_3) corresponds to an equilibrium for $b = b_0$, then $R_i(b_0) = r_i$, $i = 1, 2, 3$

We prove the axisymmetry of the equilibrium solutions by contradiction. Suppose there is a set of distinct r_1, r_2, r_3 for $b = b_0 > 0$. Without loss of generality, assume $r_1 > r_2 > r_3$. Because $r_1 + r_2 + r_3 = 0$, we have $r_1 > 0$ and $r_3 < 0$. Consider a function

$$F(b) = r_2 R_1(b) - r_1 R_2(b) \tag{31}$$

It is clear that $F(0) = F(b_0) = 0$. To establish contradiction, we carried out detailed analysis in Ref. [115] to show that

$$\begin{aligned} 2F'(b) = {} & (r_1 - r_2)(r_2 - r_3)\langle h_2(h_3 - h_1)\rangle \\ & + (r_2 - r_3)(-r_3)\langle h_3(h_2 - h_1)\rangle \\ & + (r_1 - r_2)(r_1)\langle h_1(h_3 - h_2)\rangle > 0 \\ & \text{for } b > 0 \end{aligned} \tag{32}$$

since all the coefficients and correlation terms are positive. (32) implies that $F(b)$ is a monotonically increasing function, which contradicts with the fact $F(0) = F(b_0) = 0$.

To estabilish the number of equilibria, we select the axis of symmetry as the z-axis and use the spherical coordinates to denote the unit vector $\mathbf{u}$:

$$\mathbf{u} = (u_1, u_2, u_3) = (\sin\phi\cos\theta, \sin\phi\sin\theta, \cos\phi) \tag{33}$$

Then the Maier-Saupe potential has the expression

$$V(\phi) = -r\cos^2\phi \tag{34}$$

where $r \equiv (b/2)(3\langle\cos^2\phi\rangle - 1)$ is the Flory order parameter and satisfies the equation

$$r[1 - bf(r)] = 0 \tag{35}$$

Here the function $f(r)$ is given by

$$f(r) = \frac{\int_0^1 \omega^2(1-\omega^2)\exp(r\omega^2)\,d\omega}{\int_0^1 \exp(r\omega^2)\,d\omega} \tag{36}$$

and can be shown to have the following properties:

1. $f(0) = 2/15$
2. $0 < f(r) < 1/4$
3. $\lim_{r\to-\infty} f(r) = 0$, $\lim_{r\to\infty} f(r) = 0$
4. There exists $r^* > 0$, such that $f'(r^*) = 0$, $f'(r) > 0$ for $r < r^*$ and $f'(r) < 0$ for $r > r^*$

Then the conclusion on the number of equilibria follows immediately. More specifically,

1. For $b < b^*$, there exists one solution $r = 0$.
2. For $b = b^*$, there are two solutions: $r = 0$ and $r = r^* = 2.17828797\cdots$.
3. For $b^* < b < 15/2$, there are three solutions 0, r_1 and r_2 where r_1 is between 0 and r^*, and r_2 is bigger than r^*.
4. For $b = 15/2$, there are two solutions 0 and r_2 where r_2 is bigger than r^*.
5. For $b > 15/2$, there are three solutions 0, r_1 and r_2 where r_1 is negative and r_2 is bigger than r^*.

Here $b^* = 1/f(r^*) = 6.731486\cdots$.

In contrast, in the Doi–Hess orientation tensor theory the uniaxial equilibrium branches as functions of the concentration parameter N (inversely proportional to the temperature) are given by:[40]

$$s_0 = 0, \quad s_\pm = \frac{1 \pm 3\sqrt{1 - 8/3N}}{4} \tag{37}$$

Figure 3 depicts the isotropic–nematic phase diagram for the Maier-Saupe interactions with the Doi–Hess orientation tensor theory. It was further shown in Ref. [40] that the "oblate phase" (where the order parameter $s < 0$) is stable to uniaxial perturbations, but unstable to biaxial perturbations. Thus it is unstable. This explains why "oblate phase" is not observed in equilibrium experiment; the oblate phase turns out to play a prominent role in shear flows when there are different limit cycles (tumbling and wagging, for example) at different heights in the shear gap.

Rigorous analysis for steady state solutions with the Onsager potential is still unavailable. The main difficulty lies in the fact that the Onsager potential depends on the whole function of the probability density whereas the Maier-Saupe potential depends only on the second moment.

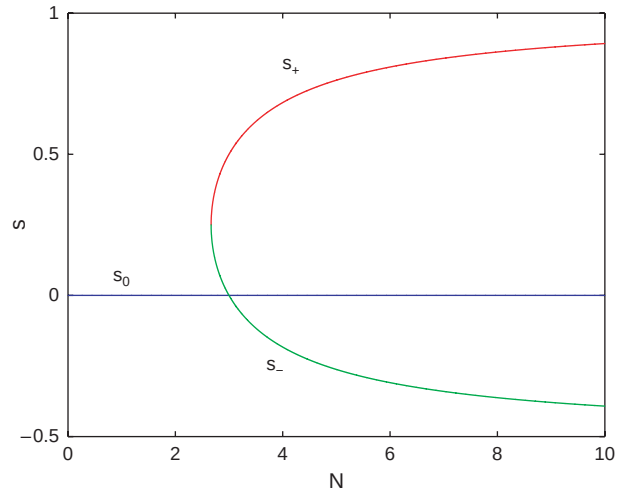

Fig. 3. Isotropic–nematic phase diagram for the Maier-Saupe intermolecular potential with the Doi closure tensor theory. The horizontal axis represents the strength of the nematic potential whereas the vertical axis denotes the nematic order parameter.

For extended nematics which consists of an ensemble of rigid rods with inherent dipoles, the Smoluchowski equation can be written as

$$\frac{\partial \rho}{\partial t} = D\frac{\partial}{\partial \mathbf{u}} \cdot \left(\frac{1}{k_B T} \frac{\partial U}{\partial \mathbf{u}} \rho + \frac{\partial \rho}{\partial \mathbf{u}} \right)$$
$$U(\mathbf{u}, [\rho]) = -\alpha k_B T \langle \mathbf{u} \rangle \cdot \mathbf{u} - b k_B T (\mathbf{u} \otimes \mathbf{u}) : \langle \mathbf{u} \otimes \mathbf{u} \rangle \quad (38)$$

Here α is strength of the dipole–dipole interaction. In Ref. [116] it was proved that all stable equilibria of rigid, dipolar rod dispersions are either isotropic or prolate uniaxial. It was further demonstrated that unstable non-axisymmetric equilibria exist and therefore the stability is essential in establishing the axisymmetry. A recent work by Lee et al.[72] studied dipole-induced first-order phase transitions of nano-rod monolayers where the total potential for dipolar Brownian rods in equilibrium is given by (38). It was shown that the coupling of a dipole potential to excluded volume is sufficient to re-instate a first-order phase transition of rods confined to two-dimensions. Extending the work to imposed elongational or shear flow, or a magnetic field remains to be explored.

3. EFFECTS OF FLOW FIELDS

Even though nematic liquid crystalline polymers (LCPs) have been studied for quite a long time, their technological applications remain dominated by high tensile strength fibers, such as Kevlar. This is mainly due to the intrinsic difficulty of maintaining a monodomain orientational state at the macroscopic level. Understanding the microstructural orientation state in any processing flow other than fiber spinning becomes extremely important in any future developments of LCPs as structural materials. Many numerical studies have been performed on the characterization of the shear flow behavior of LCPs based on various modeles, including the Leslie-Erickson theory,[50, 51] the Doi model,[27–29, 66, 98] and the Smoluchowski equation.[32, 33, 35, 36] These studies aimed to reproduce, explain and predict experimental discoveries of steady and transient modes. "By a combination of theory and experiment, many steady and transient shear-induced, monodomain modes have been catalogued and named primarily on the basis of director response: steady alignment with primary director either in the shear plane (*flow aligning*) or along the vorticity axis (*logrolling*); in-plane transient oscillatory (*wagging*) or rotating (*tumbling*) director modes; and out-of-plane transient director modes (*kayaking*). Complicated dynamics is also possible."[37] The effect of extensional flow and general linear planar flows has also been investigated.[31, 34, 37] The proof of limit cycles, except in a simple 2D tensor model, remains open to our knowledge in 3D tensor models and in either 2D or 3D kinetic equations.

We are now going to impose physical boundary conditions on the oppositely moving, steady phates. This will necessarily lead to spatial structure in the orientation field, and thereby generate nonlinear shear flow and potentially higher dimensional structures and flows. For the Doi–Hess mesoscopic orientation tensor model, the asymptotic, one-dimensional gap structures, along with the flow-gradient direction, in "slow" Couette cells were derived in Ref. [42]. A simple geometric setup of this study is sketched in Figure 4.

The scaling properties of steady flow molecular structures in slow Couette flows with equal elasticity constants in Ref. [42] were later generalized in several ways to contrast isotropic and anisotropic elasticity and to compare Couette versus Poiseuille flow and to consider dynamics and stability of these steady states within the asymptotic model equations.[16] In Ref. [12] the classical problem of the viscoelastic response of nematic liquid crystal polymers to small amplitude oscillatory shear was revisited by applying a multiple time scale pertrubation analysis to the Doi–Hess rigid rod model. The analysis in Ref. [12] was restricted to in-plane orientational configuration. Generalization of the analysis to full tensor degrees of freedom leads to a five-dimensional dynamical system, which is not yet analytically solved. In Ref. [71] monolayer films of liquid crystalline polymers were modelled with a mesoscopic two-dimensional analogue of the Doi–Hess tensor model. The weak-shear steady and unsteady selection criteria for 2D nematic polymers using various second-moment closures was derived. A simple proof was given based on the Poincare-Bendixon Theorem to show that limit cycles ("tumbling orbits") exist beyond the parameter boundary for the steady–unsteady transition. Finally, it was revealed that the shear-perturbed 2D phase diagram is significantly robust to closure approximations than the 3D system.

The effect of homogeneous elongational flows $\mathbf{v} = \nu(-x/2, -y/2, z)$ ($\nu > 0$: axially stretching; $\nu < 0$: planar stretching) was studied in Ref. [41] using the Doi–Hess orientation tensor model. All flow-induced steady states (both uniaxial and biaxial) and their stability were investigated. The main conclusions were that in axial stretching, biaxial steady state solutions exist but they are all unstable and the only stable solutions are uniaxial; in planar

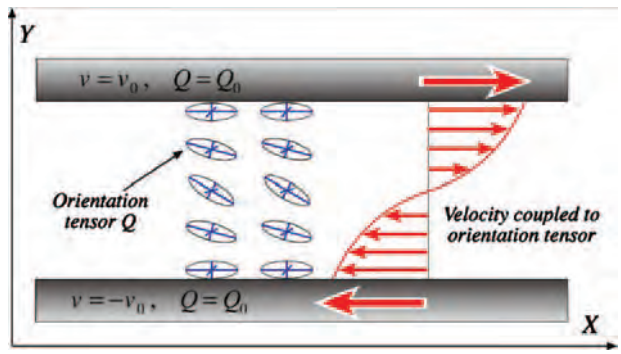

Fig. 4. A schematic diagram of the Couette cell, with no slip velocity conditions and tangential anchoring at the plates.

stretching, above a moderate concentration, the only stable solutions are biaxial.

For the Smoluchowski equation, theoretical analysis becomes more challenging. The first elegant analysis of the isotropic-to-nematic phase transition for two-dimensional liquid crystal polymers at high shear rates was given by Marrucci and Maffettone.[82, 83] In Ref. [120] the dynamics and steady states of 2-D nematic polymers driven by the weak shear were studied. We briefly review the results in 120. For polymer rods in the two-dimensional space, the orientation of a polymer rod can be described by an angle θ and the orientation direction can be represented by the unit vector $\mathbf{u} = (\cos\theta, \sin\theta)$. In the presence of a weak shear flow $\mathbf{v} = \gamma(0, -x)$, the orientation distribution function evolves according to the Smoluchowski equation

$$\begin{aligned} \frac{\partial \rho}{\partial t} &= D\frac{\partial}{\partial \theta}\left[\left(-\frac{\varepsilon}{2} + \frac{\varepsilon}{2}V'_{SH}(\theta) + V'_{MS}(\theta)\right)\rho + \frac{\partial \rho}{\partial \theta}\right] \\ V_{MS}(\theta) &= -U\langle \cos 2(\theta-\alpha)\rangle \cos 2(\theta-\alpha) \\ V_{SH}(\theta) &= \frac{1}{2}\sin 2\theta \end{aligned} \tag{39}$$

where ε is the ratio of the shear rate (γ) and rotational diffusivity (D) and is called the *Peclet number*, U is the normalized polymer concentration.

In the 2-D case, it is well-known that in the absence of flow the isotropic–nematic phase transition occurs at $U = 2$. In the presence of an imposed weak shear there is a threshold ($U_0 \approx 2.41144646$) for U: When $U < U_0$, steady state solution exists; otherwise there is no steady state. The slow time evolution driven by the weak shear can be captured by the multi-scale analysis. It was revealed in Ref. [120] that the order parameter of the orientational distribution of rodlike molecules is time invariant while the director changes with time. More specifically,

- The director of the orientational distribution converges to a stable steady state position when the strength of the nematic potential U is less than U_0.
- The angular velocity of the director is position-dependent and is always positive when the orientational distribution is temporarily periodic ("tumbling") and can never reach a steady state when U is larger than the threshold U_0.

Recently a comprehensive study of the 2-D nematic liquid crystal polymers under an arbitrary shear was provided in Ref. [107]. The study shows that when the concentration parameter U is smaller than a critical value U_0, the stable branch and an unstable branch form a fold and are connected at U_0 and it resolves the details of the transition occurs around the folding point of the phase curve. As the Peclet number increases, the stable branch and the unstable branch of the fold are peeled off from each other and are separated. When the Peclet number is larger than 0.746, the fold disappears completely and there is only one steady state for each value of U.

The effect of elongational perturbations on nematic liquid crystal polymers under a weak shear based on the two-dimensional Smoluchowski equation was investigated in Ref. [118]. Let $\mathbf{u} = (\cos\theta, \sin\theta)$ represent the orientation of rodlike molecules, $\mathbf{v} = \gamma(0, -x)$ be the shear flow, $\mathbf{v}_E = (\gamma/2)q(-y, -x)$ be the elongational perturbation. Then the Smoluchowski equation for the orientational distribution function can be written as

$$\begin{aligned} \frac{\partial \rho}{\partial t} &= D\frac{\partial}{\partial \theta}\left[(V'_{PS}(\theta) + V'_{MS}(\theta))\rho + \frac{\partial \rho}{\partial \theta}\right] \\ V_{MS}(\theta) &= -U\langle \cos 2(\theta-\alpha)\rangle \cos 2(\theta-\alpha) \\ V_{PS}(\theta) &= -\frac{\varepsilon}{2}\theta + \frac{\varepsilon}{4}(1+q)\sin 2\theta \end{aligned} \tag{40}$$

where ε is the Peclet number. Applying the multi-scale analysis, we found that

- When the elongational perturbation is very small, the orientational probability density function tumbles periodically only in an intermediate range of polymer concentrations; outside this immediate range the orientational probability density function converges to a steady state and the tumbling is arrested.
- When the elongational perturbation is increased further (by about 20% of the shear rate), the intermediate range of tumbling disappears and the orientational probability density function converges to a steady state regardless of the polymer concentration.

These findings are consistent with various earlier results based on the Leslie-Ericksen theory[10] or analogous 3D numerical simulations.[43] It is worthwhile to point out that even though the rigor of multi-scale asymptotic analysis has not yet been established, the method itself has become a powerful mathematical tool in recent applications. For example, Choate and Forest[12] applied it to study the viscoelastic response of nematic polymers to small amplitude oscillatory shear; Vicente Alonso et al.[102] used it to investigate the nonlinear dynamics of a nematic liquid crystal in the presence of a plane Couette flow using a Landau-de Gennes model; Chillingworth et al.[11] employed it to describe the geometry and dynamics of nematic liquid crystal in a uniform shear flow.

In summary, the analytical studies of the Smoluchowski equation for nematic liquid crystal polymers under shear, elongational, or other simple planar linear flows have been limited to relatively simple two-dimensional case. Very recently Zhang and Zhang[111] provided a theoretical study on stable equilibria of liquid crystals without flow and the stable dynamic states for nematic liquid crystals under weak shear flow for the Smoluchowski equation. Semi-analytical results on the Smoluchowski equation with the Onsager potential are provided in Ref. [105]. Extensions to general shear flow and general linear planar flow remain unexplored.

4. NANOCOMPOSITES AND EFFECTIVE CONDUCTIVITY

One particular area of nanotechnology research has been carbon nanotubes (CNTs). Ever since their discovery in 1991, nanotubes have emerged as stars of the chemistry world. They are stronger than steel, lightweight, and able to withstand repeated bending, buckling, and twisting; they can conduct electricity as well as copper or semiconduct like silicon; and they transport heat better than any other known material. CNTs can be thought of as a sheet of graphite, which has its two ends wrapped together to form a hollow cylinder and has a cap enclosing the tube at one of the ends. CNTs exhibit a high aspect ratio (length-to-diameter ratio), with the length generally several μm and the diameter approximately 0.4 to 100 nm. Nano-elements like CNTs are combined at low (0.1–5%) volume fractions with traditional polymeric materials to enhance a diverse set of targeted properties. Notable examples include high electrical conductivity and strength of CNTs and the barrier properties of nano-clay platelets. Nanoparticle suspensions, ranging from DNA, viruses and carbon nanotubes to mineral suspensions with rod-or disk like particles also form liquid crystal phases, as do micron-sized colloidal particles in solvents.

Recently Zheng et al.[112] applied homogenization theory to predict the effective conductivity tensor, σ^e, for uniform suspensions of ellipsoidal nano-inclusions of rigid rods with conductivity σ_2 and volume fraction θ_2 in a matrix of conductivity σ_1. For simplicity, all ellipsoids are assumed to have the same geometry with three semi-axes a, b and c ($a > b = c$ for spheroidal rods and $a = b > c$ for spheroidal platelets). The ellipsoids orient due to excluded-volume interactions and flow according to a orientation probability distribution that is the central oject of the Doi–Hess kinetic theory. From homogenization theory of composites with spheroidal inclusions at low volume fractions, conductivity obeys elliptic equations which are virtually identical for thermal, electric, and dielectric properties. The effective conductivity tensor in close form is derived in Ref. [112]:

$$\sigma^e = \sigma_1\mathbf{I} + \sigma_1\theta_2(\sigma_2-\sigma_1)\left\{\frac{2}{\sigma_2+\sigma_1-(\sigma_2-\sigma_1)L_a}\mathbf{I} + \frac{(\sigma_2-\sigma_1)(1-3L_a)}{[(\sigma_2+\sigma_1)-(\sigma_2-\sigma_1)L_a][\sigma_1+((\sigma_2-\sigma_1)L_a]}\mathbf{M}(\rho)\right\} + O(\theta_2^2) \quad (41)$$

where $\mathbf{I}$ is the 3 by 3 identity matrix, L_a is the spheroidal depolarization factor depending on the aspect ratio r ($r = a/b \gg 1$, rods; $r = c/a \ll 1$, platelets) of the molecular spheroids through the relation

$$L_a = \frac{1-\epsilon^2}{\epsilon^2}\left[\frac{1}{2\epsilon}\ln\left(\frac{1+\epsilon}{1-\epsilon}\right)-1\right], \quad \epsilon = \sqrt{1-r^{-2}} \quad (42)$$

Here ρ is the orientation probability distribution function of quiescent or flowing anisotropic macromolecules, governed by the Smoluchowski equation of the Doi–Hess kinetic theory for quiescent or flowing nematic polymers; $\mathbf{M}(\rho)$ is the second-moment of the orientation probability density ρ. From the closed form, the scaling properties of enhanced conductivity versus volume fraction and weak shear rate become explicit. Not surprisingly, the effective conductivity tensor inherits all the features of the orientation tensor from the isotropic–nematic phase transition, including hysteresis, bi-stability, and discontinuous jumps.

In Ref. [113] we combined two classical mathematical asymptotic analysis, slender longwave hydro-dynamics[30, 41] and homogenization theory for composites,[112] to predict elongational flow enhancements in conductivity of LCP nano-composites. We found that elongational flow dominates free surface and thermal effects on electrical and thermal conductivity enhancement and there is no sacrifice in these properties by producing much larger radius fibers.

Even though the above studies are restricted to bulk homogeneous mesophases of nematic nanocomposites at rest and in weak shear flows[112] and in elongational flow,[113] they serve as benchmarks and lay the groundwork for future extensions to heterogeneity, more general flow rates and flow type, and the incorporation of effects of the "interphase" between the matrix and nano-inclusions.

5. NUMERICAL SIMULATIONS

As we have seen already, the governing equations for liquid crystal polymers (and other complex fluids) are nonlinear and the only feasible way of comparing model predictions with experimental observations is to carry out numerical simulations. In 1990 Larson[68] carried out one of the earliest numerical simulations based on the kinetic Doi–Hess model with the Onsager potential. He solved the Doi equation for the three-dimensional time-dependent orientation distribution function for rodlike nematic polymers by an expansion in spherical harmonic functions. His results confirmed two-dimensional calculations with the Maier-Saupe potential[82] and also predicted negative first normal stress difference, which is in qualitative agreement with the experimentally measured values. Later in 1991 Larson and Öttinger[70] used two numerical techniques to solve the Doi equation with the Onsager potential again. One of their numerical techniques is based on spherical harmonic function expansions, and the other is a stochastic simulation technique which basically rewrites the Doi diffusion equation as a stochastic differential equation for the time evolution of the Markovian process and then integrates the equations of motion for a large ensemble of molecules. They predicted flow-aligning, log-rolling, wagging, tumbling and kayaking. As noted earlier, the ability to detect bifurcations among these various different orbits is beyond current methods of stochastic differential equations.

In recent years the spherical harmonics expansion method has gained popularity in solving the kinetic Doi–Hess equation. For example, Grosso, Keunings, Crescitelli and Maffettone used it in their prediction of chaotic dynamics in sheared liquid crystalline polymers.[46] Forest's group[31–37] carried out more detailed monodomain studies using the spherical harmonic expansions, both for monodomains and for spatially heterogeneous nematic polymer flows.

Another popular approach to model liquid crystalline polymers is to solve the Doi tensor model instead of the Smoluchowski equation. As we mentioned in the Introduction, the Doi tensor model is an approximation of the Doi–Hess kinetic model with the the Maier-Saupe potential and the Doi-Marrucci-Greco potential. The Doi-Marrucci-Greco potential couples the Maier-Saupe short range intermolecular potential to a long range potential to account for non-local elastic interactions. The Doi-Marrucci-Greco potential is given by

$$\Phi_{DMG} = -\frac{3}{2}Uk_{\mathrm{B}}T\left(\mathbf{Q}+\frac{l^2}{24}\Delta\mathbf{Q}\right):\mathbf{mm} \qquad (43)$$

where l is the persistence length of the non-local distortional elasticity interaction and U is a constant representing the nematic strength. Calculations based on the Doi tensor model have been extensively carried out. For example, in Ref. [66] the orientation tensor is restricted to be a two-by-two matrix and the coupled flow calculations are one-dimesional, in Ref. [61] the behavior of the Doi-Marrucci-Greco (DMG) model for nematic liquid crystalline polymers in planar shear flow is investigated where the 2D assumption of no spatial gradients in the flow direction is retained in the computations. It was found in Ref. [61] that the DMG model was able to capture dynamic behaviors in accordance with experimental observations[69] for the Ericksen number and Deborah number cascades. For increasing shear rates within the Ericksen number cascade, where gradient elasticity is the dominant stress contribution, the DMG model exhibits four distinct flow regimes: stable simple linear shear flow at low shear rates; stable roll cells at intermediate shear rates; irregular structure followed by large-stain disclination formation and irregular structure preceded by disclination formation at high shear rates. For increasing shear rates within the Deborah number cascade, where the dominant contribution to the stress is viscoelasticity, the DMG model displays a stream-wide banded texture, in the absence of roll cells and disclinations, followed by a shear alignment where the mean orientation lies within the shear plane throughout the monodomain. Very recently Klein et al. extended their calculations[61] to three-dimensional shear-driven dynamics to study polydomain textures and disclination loops in liquid crystalline polymers.[62]

Finally, we want to point out that numerical simulations based on the Leslie-Ericksen theory on liquid crystals have also been carried out extensively. For example, Rey and his co-workers[50, 51] have used this theory to study bifurcation and banded textures of nematic polymers in simple shear flows. Very recently they have conducted a nanoscale analysis with a continuum theory to predict a new defect-forming mechanism for liquid crystal interfaces.[108]

6. CONTROLLABILITY AND OBSERVABILITY OF NEMATIC LIQUID CRYSTALS

The controllability of viscoelastic fields is a fundamental concept that defines some essential capabilities and limitations of the resulting materials. In practice, the shape of an extrudate can be controlled by varying the size or shape of an orifice, whereas the advance of the free surface can be controlled by varying the inflow into a mold. There is still a big gap between theoretical work and practical problems. An important issue of controllability is the question whether it is possible to steer a system to a desirable state with a given set of control inputs.

In Ref. [89] the controllability of flows of linear viscoelastic fluids was investigated by Renardy using multi-mode Maxwell models. The state of the system is characterized by the velocities and the viscoelastic stresses; the control input is in the form of the body force. It was found that the system is uncontrollable, unless the initial conditions for the stresses satisfy a set of constraints. For the degenerate case of creeping flow where the density is zero in the equation of motion, there is no controllability unless the control input is distributed along the entire interval in the physical domain. In the presence of inertia, crucial difference occurs between the cases of one or more relaxation modes: For a single relaxation mode (i.e., a Maxwell fluid), exact controllability holds provided the time interval satisfies certain inequality; for multiple relaxation modes, exact controllability holds under modified regularity assumptions. Another piece of work by Renardy[90] was focused on the homogeneous shear flow of viscoelastic fluids with several different constitutive models. For those equations, the state of the system consists of viscoelastic stresses whereas the shear rate is regarded as a control input. For the upper convected Maxwell (UCM) model, it was revealed in Ref. [90] that the reachable set, i.e., the states in stress space which are accessible from a given initial condition, is specified by a positive definiteness inequality of the stress tensor. Very recently the result was extended to the control of nonhomogeneous shear flow of an upper convected Maxwell fluid[91] where the state of the system and the available control are the same as those in Ref. [89]. In our very recent studies[121] we started to apply nonlinear geometric control theory to examine the controllability of the upper convected Maxwell model under various homogeneous flows. In Ref. [121] we adopted a local version of the concept, namely weak controllability. This definition has been widely used in nonlinear control theory as well as in engineering applications. In many real life

applications of complicated nonlinear systems, engineers prefer to reach a distance target by scheduling a sequence of local movements for the reasons of model uncertainties, system perturbations, and sensor noise.

In the following we present on overall basic definition and description of *weak controllability* adopted from Ref. [55].

Let

$$\dot{x} = f(x) + \sum_{i=1}^{m} g_i(x) u_i \tag{44}$$

be a general nonlinear control system, where x is the state variable, and $u_i \in \Re$, $i = 1, \ldots, m$, are the control variables. Let M denote the manifold of state variables. A point x_1 in M is *reachable* from a point x_0 in M if there exist piecewise continuous input functions, $u_i = \alpha_i(t)$, such that the trajectory, $x(t)$, of (44) with initial state x_0 reaches x_1 in finite time. The global reachability is usually hard to prove for nonlinear control systems. A feasible solution is to seek weak controllability. The system (44) is *weakly controllable* within some open subset $S \subseteq M$ if for each point $x_0 \in S$, there is an open neighborhood U_0 of x_0 so that the set of points reachable from x_0 along trajectories inside U_0 contains at least an open subset of M.

A powerful sufficient condition on the weak controllability of a nonlinear control system is the contollability rank condition (CRC).[55] Namely, a control system of the form (44) is weakly controllable on an open set S if it satisfies the controllability rank condition on S, i.e.,

$$dim(\Delta_{\mathscr{C}}(x)) \equiv n \tag{45}$$

for all $x \in S$, where n is the dimension of the manifold M, and

$$\Delta_{\mathscr{C}}(x) = \text{span}\{X(x) \mid X \text{is a vector field in the control Lie algebra}\}.$$

From a theoretical viewpoint, Lie brackets of vector fields provide an efficient tool to prove weak controllability.

The study in Ref. [121] can be extended to the nematic liquid crystal polymers using the Doi–Hess tensor theory. As a toy model, let us consider the two-dimensional Doi model with imposed extensional flow.

For a homogeneous extensional flow with rate $\dot{\gamma}(t)$, the velocity is

$$\mathbf{v} = \dot{\gamma}(t)\left(\frac{x}{2}, -\frac{y}{2}\right) \tag{46}$$

The rate-of-strain tensor becomes

$$\mathbf{D} = \frac{1}{2}[\nabla\mathbf{v} + (\nabla\mathbf{v})^T] = \frac{\dot{\gamma}(t)}{2}\begin{bmatrix} 1 & 0 \\ 0 & -1 \end{bmatrix} \tag{47}$$

The Doi tensor model for nematic liquid crystalline polymer under extensional flow is given by

$$\frac{d}{dt}\mathbf{Q} = \Omega\mathbf{Q} - \mathbf{Q}\Omega + a[\mathbf{D}\mathbf{Q} + \mathbf{Q}\mathbf{D}] + a\mathbf{D} - 2a\mathbf{D} : \mathbf{Q}(\mathbf{Q} + \mathbf{I}/2) - 6D_r F(\mathbf{Q}) \tag{48}$$

where

$$\mathbf{Q} = \begin{bmatrix} Q_{11} & Q_{12} \\ Q_{12} & -Q_{11} \end{bmatrix} \text{ is the orientation tensor,}$$
$$\Omega = \frac{1}{2}[\nabla\mathbf{v} - (\nabla\mathbf{v})^T] \text{ is the vorticity tensor,} \tag{49}$$
$$F(\mathbf{Q}) = \left(1 - \frac{N}{2}\right)\mathbf{Q} - N\mathbf{Q}^2 + N\mathbf{Q} : \mathbf{Q}\left(\mathbf{Q} + \frac{\mathbf{I}}{2}\right)$$

a is a dimensionless parameter depending on the molecular aspect ratio, N is a dimensionless concentration of nematic polymers, D_r is an averged rotary diffusivity or relaxation rate. After some rescaling and nondimensionalization, the nematodynamic model (48) can be written as

$$\frac{d\vec{x}}{dt} = \vec{f}(\vec{x}) + \vec{g}(\vec{x})u$$

where

$$\vec{x} = \begin{bmatrix} x_1 \\ x_2 \end{bmatrix} = \begin{bmatrix} Q_{11} \\ Q_{12} \end{bmatrix},$$
$$\vec{f}(\vec{x}) = -6\left[1 - \frac{N}{2} + 2N(x_1^2 + x_2^2)\right]\vec{x}, \tag{50}$$
$$\vec{g}(\vec{x}) = \begin{bmatrix} a\left(\frac{1}{2} - 2x_1^2\right) \\ -2ax_1x_2 \end{bmatrix}, \quad u = Pe(t)$$

We now regard $Pe(t)$ as a control input and consider the problem (50) with initial state $\mathbf{Q}_0$ and final state $\mathbf{Q}_1$. The system is controllable if for any choices of $\mathbf{Q}_0$ and $\mathbf{Q}_1$, there exists a control $Pe(t)$ on the interval $(0, T)$.

The Lie bracket is calculated to be

$$[\vec{f}, \vec{g}] = \begin{bmatrix} 6a\left\{2x_1^2\left[1 - \frac{N}{2} - 2N(x_1^2 + x_2^2)\right] + \frac{1}{2} - \frac{N}{4} + N(3x_1^2 + x_2^2)\right\} \\ 12ax_1x_2\left[1 + \frac{N}{2} - 2N(x_1^2 + x_2^2)\right] \end{bmatrix}$$

Finally, we have

$$\det[\vec{g}, [\vec{f}, \vec{g}]] = 12a^2x_1x_2 \tag{51}$$

The determinant does not equal zero when $x_1 \neq 0$ and $x_2 \neq 0$. So the Doi model (50) under extensional flow satisfies CRC and is weakly controllable when $Q_{11} \neq 0$ and $Q_{12} \neq 0$. In terms of geometric words, the system (50) is weakly controllable at all points in $R^2 \backslash \{S_1 \cup S_2\}$ where

$$R^2 = \{(x_1, x_2) \mid x_1, x_2 \in R\}, \quad S_1 = \{(x_1, x_2) \mid x_1 = 0\},$$
$$S_2 = \{(x_1, x_2) \mid x_2 = 0\}$$

Extending the above preliminary study to 3-D orientation tensor theory and other flow geometries (e.g., shear flow) and finding reachable set remain to be explored.

REVIEW

The observability of nematic liquid crystal polymers is still open. Roughly speaking, by observability we mean the ability to determine the orientation distribution or orientation tensor of nematic polymers from the time history of the observations. The observations can vary, for example, the birefringence measurements from light scattering experiments. Recently Krener[65] studied the observability of one and two-point two-dimensional vortex flow from one or two Eulerian and Lagrangian observations. In his work, an Eulerian observation is a measurement of the velocity of the flow at a fixed point in the domain of the flow whereas a Lagrangian observation is a measurement of the position of a particle moving with the fluid. By applying the observability and strong observability rank conditions and calculating them for different vortex configurations and observations, it was found that vortex flows with Lagrangian observations tend to be more observable than the same flows with Eulerian observations. Extending this work on vortex flows to complex flows including nematic liquid crystal polymers is practically important.

7. OTHER DIRECTIONS

Other current and future research directions of nematic liquid crystals include theoretical and numerical studies of biaxial liquid crystals whose molecules are ellipsoidal, brick-shaped, V-shaped, bow-shaped, boomerang-shaped or banana shaped.[76] Recall that in a nematic phase the molecules tend to align along the director **n**. A biaxial nematic phase may result due to the further breaking of the rotational symmetry of the system around the director **n**. The existence of the biaxial nematic phase was originally predicted theoretically[45] and later observed experimentally.[78]

The equilibrium phase diagram of a class of biaxial nematic liquid crystals was given in Refs. [5, 99] using mean field theories with a generalized Straley's interaction potential. Very recently shear induced mesostructures (either steady or time-dependent) in biaxial liquid crystals were reported in Ref. [97] using a hydrodynamical kinetic theory where the governing Smoluchowski equation was solved numerically with the Galerkin method. In Ref. [97] the simple plane shear flows were used. Extending this to more complicated flows remains to be explored.

8. CONCLUDING REMARKS

In this review we have briefly summarized recent theoretical and numerical studies on liquid crystal polymers. Some unexplored problems and areas which need future attention have been identified. Due to its complexity and importance, this field will inspire and involve more scientific activities.

Acknowledgments: This work was partially supported by the Air Force Office of Scientific Research, the National Science Foundation, and the Army Research Office.

References

1. B. D. Bedford and W. R. Burghardt, *J. Rheol.* 40, 235 **(1996)**.
2. A. N. Beris and B. J. Edwards, Thermodynamics of Flowing Systems, Oxford University **(1994)**.
3. R. B. Bird, R. C. Armstrong, and O. Hassager, Dynamics of Polymeric Fluids, 2nd edn., John Wiley and Sons, New York **(1987)**, Vol. 1.
4. R. B. Bird, C. F. Curtiss, R. C. Armstrong, and O. Hassager, Dynamics of Polymeric Fluids, 2nd edn., John Wiley and Sons, New York **(1987)**, Vol. 2.
5. F. Bisi, E. G. Virga, E. C. Gartland, G. De Matteis, A. M. Sonnet, and G. E. Durand, *Phys. Rev. E.* 73, 051709 **(2006)**.
6. W. Burghardt, *Macromol. Chem. Phys.* 199, 471 **(1998)**.
7. M. C. Calderer and B. Mukherjee, *J. Rheol.* 42, 1519 **(1998)**.
8. C. V. Chaubal, L. G. Leal, and G. H. Fredrickson, *J. Rheol.* 39, 73 **(1995)**.
9. C. V. Chaubal, A. Srinivasan, O. Egecioglu, and L. G. Leal, *J. Non-Newtonian Fluid Mech.* 70, 125 **(1996)**.
10. C. V. Chaubal and L. G. Leal, *J. Non-Newtonian Fluid Mech.* 82, 25 **(1999)**.
11. D. Chillingworth, E. V. Alonso, and A. Wheeler, *J. Phys. Soc. Jpn.* 34, 1393 **(2001)**.
12. E. P. Choate and M. G. Forest, *Rheol. Acta* 46, 83 **(2006)**.
13. P. Constantin, I. Kevrekidis, and E. S. Titi, *Arch. Rat. Mech. Anal.* 174, 365 **(2004)**.
14. P. Constantin, I. Kevrekidis, and E. S. Titi, *Discrete Continuous Dynam. Syst.* 11, 101 **(2004)**.
15. P. Constantin and J. Vukadinovic, *Nonlinearity* 18, 441 **(2005)**.
16. Z. Cui, M. G. Forest, Q. Wang, and H. Zhou, *SIAM J. Appl. Math.* 66, 1227 **(2006)**.
17. L. R. P. de Andrade Lima and A. D. Rey, *J. Rheol.* 47, 1261 **(2003)**.
18. L. R. P. de Andrade Lima and A. D. Rey, *J. Non-Newtonian Fluid Mech.* 110, 103 **(2003)**.
19. L. R. P. de Andrade Lima and A. D. Rey, *J. Rheol.* 48, 1067 **(2004)**.
20. P. G. de Gennes, The Physics of Liquid Crystals, Oxford University **(1974)**.
21. C. Denniston, E. Orlandini, and J. M. Yeomnans, *Comput. Theor. Polym. Sci.* 11, 389 **(2001)**.
22. A. M. Donald, A. H. Windle, and S. Hanna, Liquid Crystalline Polymers, 2nd edn., Cambridge University Press **(2006)**.
23. M. Doi and S. F. Edwards, Theory of Polymer Dynamics, Oxford University Press, Clarendon **(1986)**.
24. J. L. Ericksen, Advances in Liquid Crystals, edited by G. H. Brown, Academic, New York **(1976)**, pp. 233–298.
25. I. Fatkullin and V. Slastikov, *Nonlinearity* 18, 2565 **(2005)**.
26. I. Fatkullin and V. Slastikov, *Commun. Math. Sci.* 3, 21 **(2005)**.
27. J. Feng, J. Tao, and L. G. Leal, *J. Fluid Mech.* 449, 179 **(2001)**.
28. J. Feng, C. V. Chaubal, and L. G. Leal, *J. Rheology* 42, 1095 **(1998)**.
29. J. Feng, G. Sgalari, and L. G. Leal, *J. Rheol.* 44, 1085 **(2000)**.
30. M. G. Forest, H. Zhou, and Q. Wang, *Adv. Polym. Tech.* 18, 314 **(1999)**.
31. M. G. Forest, R. Zhou, and Q. Wang, *Phys. Rev. E* 66, 031712 **(2002)**.
32. M. G. Forest, Q. Wang, and R. Zhou, *Rhelogoical Acta* 44, 80 **(2004)**.

33. M. G. Forest, R. Zhou, and Q. Wang, *Rheological Acta* 43, 17 (**2004**).
34. M. G. Forest, R. Zhou, and Q. Wang, *Phys. Rev. Lett.* 93, 088301 (**2004**).
35. M. G. Forest, R. Zhou, and Q. Wang, *SIAM MMS* 3, 853 (**2005**).
36. M. G. Forest, R. Zhou, and Q. Wang, *J. Non-Newtonian Fluid Mech.* 116, 183 (**2004**).
37. M. G. Forest and Q. Wang, *Rheol. Acta* 42, 20 (**2003**).
38. M. G. Forest, S. Sircar, Q. Wang, and R. Zhou, *Phys. Fluids A* 18, 103102 (**2006**).
39. M. G. Forest, Q. Wang, and H. Zhou, *J. Rheol.* 43, 1573 (**1999**).
40. M. G. Forest, Q. Wang, and H. Zhou, *Phys. Rev. E* 61, 6655 (**2000**).
41. M. G. Forest, Q. Wang, and H. Zhou, *Phys. Fluids* 12, 490 (**2000**).
42. M. G. Forest, Q. Wang, H. Zhou, and R. Zhou, *J. Rheol.* 48, 175 (**2004**).
43. M. G. Forest, Q. Wang, R. Zhou, and E. Choate, *J. Non-Newtonian Fluid Mech.* 118, 17 (**2004**).
44. F. C. Frank, *Discussion of the Faraday Society* 25, 19 (**1958**).
45. M. J. Freiser, *Phys. Rev. Lett.* 24, 1041 (**1970**).
46. M. Grosso, R. Keunings, S. Crescitelli, and P. L. Maffettone, *Phys. Rev. Lett.* 86, 3184 (**2001**).
47. S. Hess, *Z. Naturforsch. Teil A* 30, 728 (**1975**).
48. S. Hess, *Z. Naturforsch. A* 31A, 1034 (**1976**).
49. S. Hess and M. Kroger, *J. Phys.: Condens. Matter.* 16, S3835 (**2004**).
50. W. H. Han and A. D. Rey, *Journal of Non-Newtonian Fluid Mechanics* 48, (**1993**).
51. W. H. Han and A. D. Rey, *Macromolecules* 28, 8401 (**1995**).
52. E. J. Hinch and L. G. Leal, *J. Fluid Mech.* 76, 187 (**1976**).
53. K. Hongladarom and W. R. Burghardt, *Macromolecules* 26, 785 (**1993**).
54. R. R. Huilgol, *J. Non-Newtonian Fluid Mech.* 87, 117 (**1999**).
55. A. Isidori, Nonlinear Control Systems, 3rd edn., Springer (**1995**).
56. G. Ji, Q. Wang, P. Zhang, and H. Zhou, *Phys. Fluids* 18, 123103 (**2006**).
57. G. Ji, Q. Wang, P. Zhang, H. Wang, and H. Zhou, *Communications in Mathematical Sciences* 5, 917 (**2007**).
58. R. F. Kayser and H. J. Raveche, *Phys. Rev. A* 17, 2067 (**1978**).
59. A. R. Khokhlov and A. N. Semenov, *Physica A* 108, 546 (**1981**).
60. A. R. Khokhlov and A. N. Semenov, *Physica A* 112, 605 (**1982**).
61. D. H. Klein, L. G. Leal, C. Carcia-Cervera, and H. Ceniceros, *Phys. Fluids* 19, 023101 (**2007**).
62. D. H. Klein, L. G. Leal, C. Carcia-Cervera, and H. Ceniceros, *J. Rheol.* 52, 837 (**2008**).
63. M. Kleman and O. D. Lavrentovich, Soft Matter Physics: An Introduction, Springer (**2002**).
64. M. Kleman, Points, Lines and Walls: In Liquid Crystals, Magnetic Systems and Various Ordered Media, John Wiley and Sons Inc. (**1982**).
65. A. Krener, *Tellus A* 60, 1089 (**2008**).
66. R. Kupfermann, M. Kawaguchi, and M. M. Denn, *J. Non-Newt. Fluid Mech.* 91, 255 (**2000**).
67. R. G. Larson, The Structure and Rheology of Complex Fluids, Oxford University Press (**1999**).
68. R. G. Larson, *Macromolecules* 23, 3983 (**1990**).
69. R. G. Larson and D. W. Mead, *Liq. Cryst.* 12, 751 (**1993**).
70. R. G. Larson and H. C. Öttinger, *Macromolecules* 24, 6270 (**1991**).
71. J. H. Lee, M. G. Forest, and R. Zhou, *Discrete and Continuous Dynamical Systems-Series B* 6, 339 (**2006**).
72. J. H. Lee, M. G. Forest, Q. Wang, and R. Zhou, *Phys. Lett. A* 372, 3484 (**2008**).
73. F. M. Leslie, Theory of flow phenomena in liquid crystals, Advances in Liquid Crystals, edited by G. H. Brown, Adademic, New York (**1979**), pp. 1–81.
74. F. H. Lin and C. Liu, *Journal of Partial Differential Equations* 14, 289 (**2001**).
75. H. L. Liu, H. Zhang, and P. W. Zhang, *Communcations in Mathematical Sciences* 3, 201 (**2005**).
76. T. C. Lubensky and L. Radzihovsky, *Phys. Rev. E* 66, 031704 (**2002**).
77. C. Luo, H. Zhang, and P. Zhang, *Nonlinearity* 18, 379 (**2005**).
78. L. A. Madsen, T. J. Dingemans, M. Nakata, and E. T. Samulski, *Phys. Rev. Lett.* 92, 145505 (**2004**).
79. P. L. Maffettone and S. Crescitelli, *J. Rheol.* 38, 1559 (**1994**).
80. W. Maier and A. Saupe, *Z. Naturforsch A* 14A, 882 (**1959**).
81. G. Marrucci and F. Greco, *Adv. Chem. Phys.* 86 (**1993**).
82. G. Marrucci and P. L. Maffettone, *Macromolecules* 22, 4076 (**1989**).
83. G. Marrucci and P. L. Maffettone, *J. Rheol.* 34, 1217 (**1990**).
84. P. Mather, A. Romo-Uribe, C. D. Han, and S. Kim, *Macromolecules* 30, 7977 (**1997**).
85. T. Maruyama, G. G. Fuller, M. Grosso, and P. L. Maffettone, *J. Non-Newtonian Fluid Mech.* 76, 233 (**1998**).
86. H. Nijmeijer and A. J. van der Schaft, Nonlinear Dynamical Control Systems, Springer (**1990**).
87. L. Onsager, *Ann. N. Y. Acad. Sci.* 51, 627 (**1949**).
88. P. Palffy-Muhoray, *Physics Today* 60, 54 (**2007**).
89. M. Renardy, *Systems & Control Letters* 54, 1183 (**2005**).
90. M. Renardy, *J. Non-Newtonian Fluid Mech.* 131, 59 (**2005**).
91. M. Renardy, *Z. Angew. Math. Mech.* 87, 213 (**2007**).
92. M. Renardy, Mathematical Analysis of Viscoelastic Flows, Society for Industrial Mathematics (**1987**).
93. A. D. Rey, *Macromol. Theory Simul.* 4, 857 (**1995**).
94. A. D. Rey and T. Tsuji *Macromol. Theory Simul.* 7, 623 (**1998**).
95. A. D. Rey and M. M. Denn, *Annual Rev. Fluid Mech.* 34, 233 (**2002**).
96. S. Singh, *Physics Report* 324, 107 (**2000**).
97. S. Sircar and Q. Wang, *Phys. Rev. E* 78, 061702 (**2008**).
98. G. Sgalari, L. G. Leal, and J. Feng, *J. Non-Newt. Fluid Mech.* 102, 361 (**2002**).
99. A. M. Sonnet, E. G. Virga, and G. E. Durand, *Phys. Rev. E* 67, 061701 (**2003**).
100. M. Srinivasarao and G. C. Berry, *J. Rheol.* 35, 379 (**1991**).
101. Z. Tan and G. C. Berry, *J. Rheol.* 47, 73 (**2003**).
102. E. V. Alonso, A. Wheeler, and T. J. Sluckin, *Proc. R. Soc. London, Ser. A* 459, 195 (**2003**).
103. E. G. Virga, Variational Theories for Liquid Crystals, Chapman and Hall/CRC (**1995**).
104. Q. Wang, H. Sircar, and H. Zhou, *Comm. Math. Sci.* 3, 605 (**2005**).
105. H. Wang and H. Zhou, *Phys. Lett. A* 372, 3423 (**2008**).
106. H. Wang and P. Hofman, *Comm. Math. Sci.* 6, 949 (**2008**).
107. H. Wang, H. Zhou, and G. Forest, *Discrete and Continuous Dynamical Systems Series B* 11, 497 (**2009**).
108. B. M. Wincure and A. D. Rey, *Nano Lett.* 7, 1474 (**2007**).
109. K. S. Yim, G. G. Fuller, A. Datko, and C. Eisenbach, *Macromolecules* 34, 6972 (**2001**).
110. A. Zarnescu, *Nonlinearity* 19, 1619 (**2006**).

111. H. Zhang and P. Zhang, *Physica D* 232, 156 **(2007)**.
112. X. Zheng, M. G. Forest, R. Lipton, R. Zhou, and Q. Wang, *Adv. Funct. Mater.* 15, 627 **(2005)**.
113. H. Zhou, M. G. Forest, X. Zheng, Q. Wang, and L. Lipton, *Macromolecular Symposia* 228, 81 **(2005)**.
114. H. Zhou and M. G. Forest, *Discrete and Continuous Dynamical Systems-Series B* 6, 407 **(2006)**.
115. H. Zhou, H. Wang, M. G. Forest, and Q. Wang, *Nonlinearity* 18, 2815 **(2005)**.
116. H. Zhou, H. Wang, Q. Wang, and M. G. Forest, *Nonlinearity* 20, 277 **(2007)**.
117. H. Zhou, M. G. Forest, and Q. Wang, *Discrete and Continuous Dynamical Systems-Series B* 8, 707 **(2007)**.
118. H. Zhou and H. Wang, *Phys. Fluids* 19, 103107 **(2007)**.
119. H. Zhou, L. Wilson, and H. Wang, *Abstract and Applied Analysis* 36267, 15 **(2007)**.
120. H. Zhou and H. Wang, *Communications in Mathematical Sciences* 5, 1113 **(2007)**.
121. H. Zhou, W. Kang, A. Krener, and H. Wang, *Journal of Non-Newtonian Fluid Mechanics* 150, 104 **(2008)**.
122. R. Zhou, M. G. Forest, and Q. Wang, *SIAM Multiscale Modeling and Simulation* 3, 853 **(2005)**.

Received: 14 October 2008. Accepted: 10 December 2008.